Applied Environmental Research (2026) 48(2), 011
https://doi.org/10.35762/AER.2026011

Applied Environmental Research
- RESEARCH FOR SUSTAINABLE PLANET -

Research Article

Fabrication of Acid-modified Corn Plant By-product-based Biochar for Efficient Adsorption of Sulfamethoxazole from Aqueous Solutions

Nguyen Thi An Hang*, Le Thi Duyen, Bui Thi Hang

Master's Program in Environmental Engineering, VNU Vietnam Japan University, Hanoi, Vietnam

*Corresponding Email: nta.hang@vju.ac.vn

Abstract

Antibiotic pollution is of great interest owing to growing concerns about antibiotic resistance worldwide. This study aims to fabricate acid-modified biochar (CBM-A) from corn plant byproducts (CRs) for sulfamethoxazole (SMX) adsorption in aqueous solutions. CBM-A was synthesized via pyrolysis at 700 °C and modified with 14% H_3PO_4. Kinetics, isotherms, and thermodynamics were investigated in combination with material characterization to elucidate the adsorption behaviors and mechanisms. The results showed that pyrolysis and acid modification effectively enhanced SMX adsorption by CR because of the increased number of binding groups, specific surface area, and porosity. SMX adsorption on CBM-A was optimized at a natural pH of 6.3, initial SMX concentration of 30 mg L^{-1}, CBM-A dose of 1.5 g L^{-1}, contact time of 2 h, and temperature of 298 K. Under the optimal conditions and initial SMX concentration range of 10–200 mg L^{-1}, the maximum SMX adsorption capacity (q_{max}) of CBM-A was 63.29 mg g^{-1}. The Langmuir isotherm (R^2 = 0.9945) and Pseudo-second-order kinetic (R^2 = 0.9928) models were appropriate for describing SMX adsorption on CBM-A. The adsorption process was favorable and endothermic. Owing to its facile preparation, high q_{max} value, and short equilibrium time, CBM-A is considered a promising biosorbent for eliminating SMX from aqueous solutions.

ARTICLE HISTORY

Received: 9 Oct. 2025
Revised: 24 Jan. 2026
Accepted: 29 Jan. 2026
Published: 5 Feb. 2026

KEYWORDS

Antibiotic removal;
Sulfamethoxazole;
Corn plant byproducts;
Chemically modified biochar;
Adsorption behaviors;
Mechanisms

Introduction

Antibiotics, which are classified as emerging persistent organic pollutants (POPs), are of great interest to scientists worldwide. This is because antibiotics are broadly used in daily life for disease treatment in humans and animals. Antibiotics normally enter aquatic media via wastewater. They can accumulate in aquatic organisms and then be transferred into animals and humans via the food chain. As a result, the abuse of antibiotics can affect antibiotic resistance genes and bacteria, thereby threatening public and ecological health (Chen et al., 2018; Tran et al., 2023).

Among various existing antibiotics, sulfamethoxazole (SMX) is commonly used and has been detected to be in the range of 5.57 mg L^{-1} in shrimp ponds (Liu et al., 2023) and 10.03–11,583.33 mg L^{-1} in livestock wastewater (Choi et al., 2016). It is highly durable and has a long half-life of up to 100 days. Therefore, it poses a high risk to public health (Hou et al., 2022).

To date, many methods, such as photocatalysis, advanced oxidation, and adsorption, are available for the abatement of antibiotics in water. Adsorption has great potential, as it may offer an effective, affordable, and environmentally friendly approach. Because they are characterized by high porosity and abundant functional groups, biochar and modified biochar have promising adsorption capacities for various antibiotics. The possible mechanisms for the removal of antibiotics from water by biochar include hydrophobic interactions, electrostatic interactions, π–π electron donor–acceptor (EDA) interactions, and hydrogen bonds (Ahmed et al., 2017; Tran et al., 2023; Zhang et al., 2025). Common

methods used to modify biochar to increase SMX adsorption include chemical oxidation (Hou et al., 2022), oxidative hydrolysis (Reguyal et al., 2017), composite production (Tran et al., 2025; Heo et al., 2019; Zhang et al., 2022), and acid activation (Ahmed et al., 2017; Chen et al., 2018; Zhang et al., 2022). The modification of biochars with is a simple, effective, and environmentally benign method. According to Chen et al., (2018), the utilization of 14% H_3PO_4 as a modifying agent significantly increased the q_{max} value of SMX by swine manure-derived biochar. Moreover, H_3PO_4 has low toxicity, has a low degree of pollution risk, and can be washed easily with water. Therefore, this method was selected for use in this study to increase SMX adsorption by CB.

To the best of the authors' knowledge, thus far, mandatory legal standards for antibiotic concentrations in surface water, wastewater, or drinking water cannot be found. However, the European Medicines Agency (EMA) proposed an "action limit" of less than 10 ng L^{-1} for antibiotic concentrations in surface water. Furthermore, the current trend is to aim for levels as close to undetectable as possible (EMA, 2018; Niegowska et al., 2021). The situation is expected to improve in the future when scientific evidence and appropriate monitoring technologies become available.

This study aims to fabricate an effective and eco-friendly SMX adsorbent from corn byproducts via pyrolysis coupled with acid modification. The specific objectives include (i) investigating the factors influencing SMX adsorption (pH, adsorbent dose, time, and temperature) and (ii) exploring the adsorption behaviors and mechanisms via adsorption isotherm, kinetic, and thermodynamic studies. This study is expected to provide a viable method for SMX abatement from aqueous solutions as well as for the recycling of corn byproducts, thereby promoting a circular economy and sustainable development.

Materials and methods

1) Chemical and biomass

SMX was supplied by Sigma–Aldrich Co. SMX can be found in the form of cation (SMX^+), anion (SMX^-), and zero charge (SMX^0) molecules in aqueous solutions as a result of proton exchange at the aromatic amine (pKa_1 1.6) and sulfonamide groups (pKa_2 5.7) (Choi and Kan, 2019). The corn plant byproducts were collected in Hanoi, Vietnam, as a biomass for biochar fabrication. They were chopped into pieces of less than 4 cm, cleaned with distilled water, and dried in an oven (PR305225M, Thermo Scientific Precision, USA) at 105 °C until a constant weight was obtained. The samples were ground to pass through a 600–850 µm sieve and labeled as CR.

2) Fabrication of pristine and phosphoric acid-modified biochar

The CR was pyrolyzed at 700 °C for 2 h in a muffle furnace (CWF1200, Carbolite, England) (Peng et al., 2017). The obtained biochar was ground to pass through a 600 µm mesh sieve and denoted as CB. The CB, as pristine biochar, was modified with a 14% H_3PO_4 solution as follows: 10 g of CB was placed into 20 mL of 14% H_3PO_4 solution for 24 h at room temperature (Chen et al., 2018). Afterward, the material was rinsed with distilled water to remove residual H_3PO_4 until the pH of the supernatant was approximately 7.0. It was later dried in an oven at 105 °C until a constant weight was achieved, ground into a powder, and designated CBM-A.

3) Characterization of adsorbents

The CBM-A-SMX used in the characterization tests was CBM-A after the adsorption of SMX under the optimal conditions (pH of 4.6, initial SMX concentration of 30 mg L^{-1}, dose of 1.5 g L^{-1}, contact time of 2 h, and temperature of 298 K). The surface morphology and structures of CR, CBM-A, and CBM-A-SMX were characterized via SEM (TM4000 Plus, Hitachi, Japan) at 2 and 5 kV from 1 to 10 K magnification. The specific surface area and pore characteristics of the samples were verified via a Brunauer–Emmett–Teller (BET) instrument (Gemini VII 2390, Micromeritics, USA). The Fourier transform infrared (FTIR) spectra of CR, CBM-A, and CBM-A-SMX were recorded by an FTIR analyzer (FTIR-4600, Jasco, Japan) within the wavelength range of 400–4,000 cm^{-1}. Additionally, the point of zero charge (pH_{zpc}) of CBM-A was identified via the pH drift method (Jang et al., 2018). In addition, pristine corn plant byproduct-based biochar (CB) has not been characterized. The reason was that this study focused on the SMX adsorption capacity of the 14% H_3PO_4 acid-modified biochar (CBM-A) rather than that of CB.

4) Batch adsorption experiments

All the adsorption tests were implemented in 150 mL conical flasks covered with parafilm. Batch adsorption experiments were conducted in conical flasks containing desirable pH values, predetermined doses of CBM-A, given concentrations of SMX, predetermined contact times, and specific temperatures. The mixtures were shaken at 120 rpm on an orbital shaker (NB-T101MT, N-Biotek, South Korea). To evaluate the influence of pH on SMX adsorption by CBM-A, the pH of the initial SMX solutions was adjusted to different values ranging from 2–12 with NaOH or HCl solutions via a pH meter (S220, Mettler Toledo, China). To investigate the impact of CBM-A dosage on SMX adsorption, the CBM-A dosage was varied from 0.5 to 2 g L^{-1}. For kinetic studies, CBM-A was utilized at a concentration of 1.5 g L^{-1} in 30 mg L^{-1} SMX aqueous solution, and the samples were collected at different intervals in the range of 0–960 min

to analyze the remaining concentrations of SMX. Adsorption isotherm experiments were implemented in the SMX range of 10–200 mg L^{-1}. While the lower limit of this range (10 mg L^{-1}) simulates that in livestock wastewater (Choi et al., 2016), the upper limit of this range (200 mg L^{-1}) was used to facilitate the determination and comparison of the q_{max} value of CBM-A with that of other SMX adsorbents. This occurred because the initial SMX concentration range agrees with that used in previous studies on SMX adsorption isotherms, such as 0–80 mg L^{-1} (Zheng et al., 2013), 5–100 mg L^{-1} (Liu et al., 2025), and 100–400 mg L^{-1} (Ahsan et al., 2018). For the thermodynamic experiments, three temperatures, 288, 298, and 308 K, were used for the adsorption tests. All the samples were filtered through 0.45 µm cellulose nitrate filter paper (HAWP04700, Merck, Germany). The residual SMX concentrations in the filtrates were quantified via a UV–VIS spectrophotometer (Genesys 50, Thermo Fisher Scientific, USA) at 265 nm (Zhou et al., 2015). Each adsorption experiment was performed at least in duplicate, and the average was calculated. The SMX adsorption capacity and removal efficiency of CBM-A were calculated via the following equations (Hou et al., 2022; Tran et al., 2023).

$$q_e = (C_0 - C_e)\,V/m \quad \text{(Eq.1)}$$

where q_e (mg g^{-1}) is the SMX adsorption capacity of CBM-A at equilibrium, C_0 and C_e (mg L^{-1}) are the initial and equilibrium concentrations of SMX, respectively, V (L) is the volume of the SMX solution, and m (g) is the mass of CBM-A.

$$RE = \left((C_0 - C_e)/C_0\right) * 100 \quad \text{(Eq.2)}$$

where RE (%) is the SMX removal efficiency and C_0 and C_e (mg L^{-1}) are the initial and equilibrium concentrations of SMX in the aqueous solution, respectively.

5) Adsorption modeling

The experimental data from the kinetic tests were fitted with Pseudo-first-order (PFO) and Pseudo-second-order (PSO), which are expressed in the following equations (Jia et al., 2020; Nguyen et al., 2025).

$$\ln(q_e - q_t) = \ln q_e - k_1 t \quad \text{(Eq.3)}$$

$$1/q_t = (1/k_2 q_{e^2}) + [1/q_e]t \quad \text{(Eq.4)}$$

where q_t and q_e (mg g^{-1}) represent the SMX adsorption capacity at time t and at equilibrium, respectively; k_1 (h^{-1}) and k_2 (g mg^{-1} h^{-1}) are the rate constants of PFO and PSO, respectively; and C is the boundary layer thickness constant (Chen et al., 2018).

The experimental data from the isotherm tests were fitted by the Langmuir and Freundlich models as follows (Jia et al., 2020; Nguyen et al., 2025).

$$C_e/q_e = (C_e/q_{max}) + (1/K_L q_{max}) \quad \text{(Eq.5)}$$

$$\log q_e = 1/n \log C_e + \log K_F \quad \text{(Eq.6)}$$

where q_{max} (mg g^{-1}) represents the SMX maximum adsorption capacity of CBM-A; K_L (L mg^{-1}) represents the adsorption energy for the Langmuir model; K^F ((mg g^{-1})(L mg^{-1})$^{n^{-1}}$) represents the affinity coefficient; n represents the adsorption intensity for the Freundlich model; C_e (mg L^{-1}) represents the SMX aqueous solution concentration at the equilibrium time; and q_e (mg g^{-1}) represents the SMX adsorption capacity at equilibrium.

Results and discussion

1) Material characterization

1.1) SEM analysis

The surface morphology of CR, CBM-A, and CBM-A-SMX was verified via SEM, and the results are displayed in Figure 1. The surface of CR was relatively dense and compact, with limited visible porosity, implying a low surface area and unfavorable conditions for SMX adsorption. In contrast, the surface of CBM-A exhibited well-developed tubular channels and clearly defined pore networks with deeper cavities than those of CR did, confirming that pyrolysis followed by acid modification effectively increased the porosity and surface area of CR. However, the surface of CBM-A-SMX seemed to have fewer pores than CBM-A did, suggesting that some pores on CBM-A may be blocked or covered by SMX molecules during its retention on CBM-A. This assumption was further supported by the following BET analysis results.

1.2) BET analysis

As presented in Table 1, compared with those of CR, the BET surface area and pore volume of CBM-A considerably increased from 5.53 to 436.46 m^2 g^{-1} and from 0.0075 to 0.13 cm^3 g^{-1}, respectively. This can be explained by the impacts of pyrolysis at 700 °C and 14% H_3PO_4 acid etching of CR. The BET surface area of CBM-A (436.46 m^2 g^{-1}) was even greater than that of other modified biochars, namely, wheat straw-derived, oxide-modified biochar calcined at 700 °C (R-BC700) (294 m^2 g^{-1}) [5] and swine manure-derived, H_3PO_4-modified biochar (SCA) (319.04 m^2 g^{-1}) (Chen et al., 2018). In contrast, the pore volume of CBM-A (0.13 cm^3 g^{-1}) was lower than that of R-BC700 (0.17 cm^3 g^{-1}) (Hou et al., 2022) and SCA (0.25 cm^3 g^{-1}). Notably, after SMX adsorption, compared with CBM-A, CBM-SMX demonstrated a decreased BET surface area (376.90 m^2 g^{-1})

and pore volume (0.11 cm^3 g^{-1}), possibly due to the blockage of pores by SMX molecules after adsorption. The reduction in the specific surface area, pore volume, and pore radius of CBM-A after the adsorption of SMX confirmed that SMX could occupy some of the pores of CBM-A. The BET results are strongly supported by the SEM results, confirming that pyrolysis followed by acid modification markedly enhanced the porosity of CBM-A.

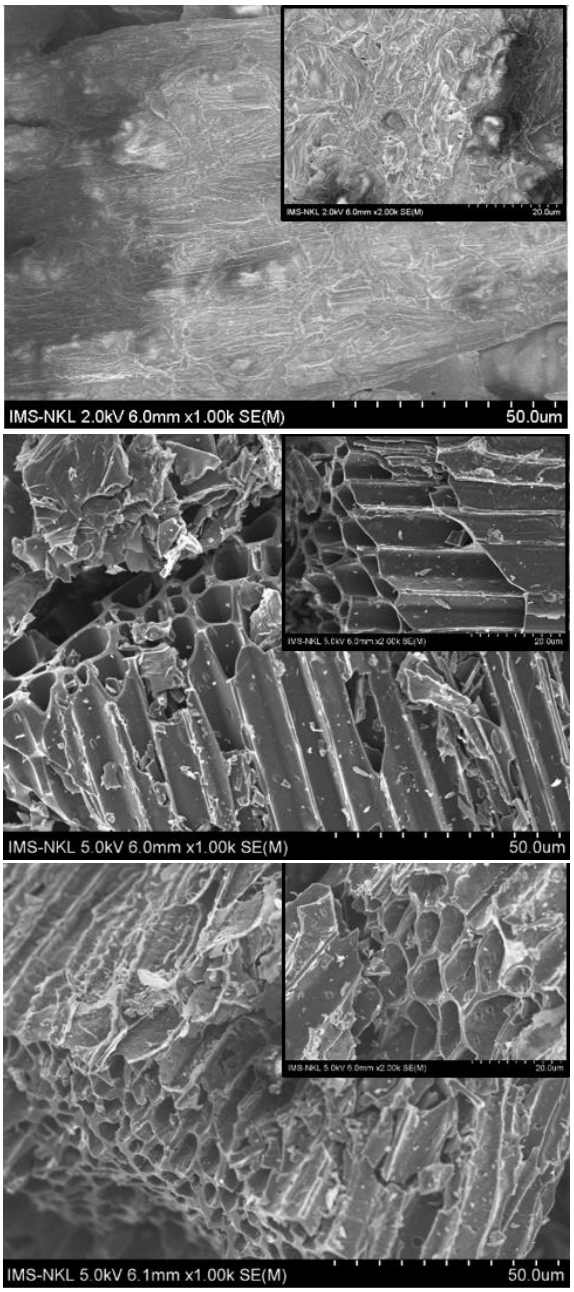

Figure 1 SEM images of a) raw corn plant byproduct (CR), b) acid-modified biochar derived from CR (CBM-A), and c) CBM-Achar after SMX adsorption (CBM-A-SMX).

1.3) FTIR analysis

The FTIR spectra of CR, CBM-A, and CBM-A-SMX are shown in Figure 2. The FTIR spectrum of CR was characterized by characteristic peaks of cellulose, such as broad O–H (3,423.73 cm^{-1}), C–H (2,922.82 cm^{-1}), C=O (1,638.87 cm^{-1}), C=C (1,426.35 cm^{-1}), and C–O (1,052.54 cm^{-1}) peaks (Choi et al., 2019; Liu et al., 2025; Taheri et al., 2024; Zhang et al., 2022). Notably, the peaks attributed to O–H (3,433.8 cm^{-1}), C=O (1,629.86 cm^{-1}), C=C (1,384.36 cm^{-1}), and C–O (1,088.15 cm^{-1}) on CBM-A shifted, indicating that SMX adsorption via these functional groups on CBM-A improved. Similar observations were reported by Tran et al. (2023) for SMX adsorption onto chitosan-biochar composites derived from agro-waste. According to Peng et al. (2017), H_3PO_4 modification added more -COOH and -OH groups to the surface of biochar. These functional groups could enhance SMX adsorption on CBM-A via H-bond formation and π–π electron–donor–acceptor (EDA) interactions (Ahmed et al., 2017; Zhang et al., 2025). In addition to electrostatic interactions and hydrogen bonding, hydrophobic interactions may also contribute to the adsorption mechanism. SMX contains aromatic and nonpolar groups that tend to associate with hydrophobic regions on the CBM-A surface. This interaction is relatively insensitive to pH and temperature changes, which may help explain the stable adsorption under varying conditions. Therefore, SMX adsorption is possibly influenced by the combined effects of hydrophobic interactions, electrostatic attraction, and other intermolecular forces (Hou et al., 2022; Sun et al., 2016). This peak is characteristic of the sulfonamide functional group in SMX, confirming the successful adsorption of SMX on CBM-A.

Table 1 BET analysis results of CR, CBM-A, and CBM-A-SMX

Parameters	CR	CBM-A	CBM-A-SMX
Specific surface area, S_{BET} (m^2 g^{-1})	5.53	436.46	376.90
Pore volume, V_p (cm^3 g^{-1})	0.0075	0.13	0.11
Pore radius, R_p (nm)	5.24	3.74	3.48

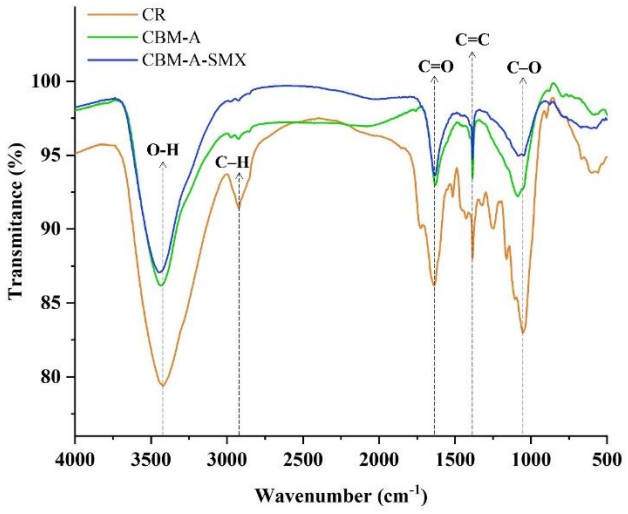

Figure 2 FTIR spectra of CR, CBM-A, and CBM-A-SMX.

2) Factors influencing sulfamethoxazole adsorption

2.1) Influence of initial solution pH

The solution pH affects SMX adsorption on CBM-A by changing the surface charge of CBM-A and the existing species of SMX. The pH_{zpc} of CBM-A was 4.6. This means that the surface of CBM-A was positively charged when the solution pH was less than 4.6; otherwise, it was negative. SMX has a pK_{a1} of 1.6 and a pK_{a2} of 5.7, which are related to a weakly acidic isoxazole heterocyclic group and an NH_2 group of the sulfonamide, respectively (Borowska et al., 2015; Choi et al., 2019). At pH < p_{Ka1} (1.6), the charge of SMX was positive. When p_{Ka1} (1.6) < pH < pK_{a2} (5.7), SMX exists in zwitterionic form, becoming nearly neutral. At pH > pK_{a2} (5.7), the charge of SMX was negative since both the heterocyclic group and the N_2 group were negative.

As illustrated in Figure 3a, the adsorption capacity of CBM-A for SMX increased in the pH range of 2–4, reached a maximum at pH 4–6.3 (44.39–46.39 mg g^{-1}), and then gradually decreased at pH 6.3–12. At pH < 1.6, SMX is positively charged, which results in electrostatic repulsion with positively charged CBM-A. In the pH range of 1.6–5.7, SMX becomes neutral, which results in low electrostatic repulsion, thereby facilitating SMX capture by positively charged CBM-A (at pH 1.6–4.6) or negatively charged CBM-A (at pH 4.6–5.7). The highest SMX adsorption capacity of CBM-A at pH 4–6.3 could be explained by nonlectrostatic interactions such as hydrogen bonding (OH groups on CBM-A and neutral SMX) and π–π interactions (C=C and C=O groups on CBM-A interact with SMX) (Choi et al., 2019; Tran et al., 2023). At pH > 5.7, the negatively charged SMX had a repulsive force with the negatively charged CBM-A, resulting in low SMX adsorption. Similarly, the maximum SMX adsorption capacity of functionalized Eucalyptus wood-based biochar (fBC) was attained at pH 4–4.25 (Ahmed et al., 2017). Since the SMX adsorption capacity of CBM-A at a natural pH (6.3) was quite similar to the highest capacity at pH 4, a natural pH of 6.3 was chosen for the next experiment.

2.2) Influence of adsorbent dose

The impact of the adsorbent dose on SMX retention by CBM-A is displayed in Figure 3b. As the CBM-A dose increased from 0.5 to 2 g L^{-1}, the SMX removal efficiency increased. This can be attributed to more active binding sites being available at a higher adsorbent dose. However, the SMX adsorption capacity decreased with increasing CBM-A dose. This is probably due to agglomeration at higher doses, causing a reduction in the active surface area of CBM-A (Tran et al., 2023). On the basis of the SMX abatement efficacy and economic viability, a CBM-A dose of 1.5 g L^{-1} was selected for the next experiments. The SMX removal efficiency and adsorption capacity were 98.18% and 20.26 mg g^{-1}, respectively. At 1.5 g L^{-1}, the removal efficiency (98.18%) was greater than that at 1.25 g L^{-1} (96.92%). Additionally, above a dose of 1.5 g L^{-1}, the SMX removal efficiency changed marginally. Therefore, a concentration of 1.5 g L^{-1} ensured more complete removal of SMX than did a concentration of 1.25 g L^{-1}.

2.3) Influence of contact time

Figure 3c shows the effect of the contact time on the SMX removal efficiency. The SMX removal efficiency (91.15%) at 120 minutes closely approached the equilibrium removal efficiency (98.78%) at 960 minutes. The difference in the SMX removal efficiency at these two contact times was negligible, suggesting that a majority of the adsorption sites were occupied in the first 120 min. This can be attributed to the substantial decrease in the number of available adsorption sites on the surface of CBM-A between the two contact times (Zhou et al., 2017). A contact time of 120 min ensures a relatively high removal efficiency, optimal contact time, and economic practical applications. Therefore, 120 min was selected for the subsequent experiments.

2.4) Influence of temperature/therrorynamics

As shown in Figure 3d, the maximum adsorption capacity (q_{max}) of CBM-A for SMX increased from 58.824 to 65.359 mg g^{-1} as the temperature increased from 288 to 308 K (Figure 3d). The thermodynamic parameters for SMX adsorption on CBM-A are given in Table 2. The negative values of ΔG indicated that the elimination of SMX by CBM-A was spontaneous. The ΔG value (1.52–3.80 kJ mol^{-1}) was in the range of 0–20 kJ mol^{-1}, suggesting that physical adsorption prevailed (Ahsan et al., 2018). Similar results were reported for SMX adsorption on chitosan-biochar composites (Tran et al., 2023). The positive values of ΔH (31.24 kJ mol^{-1}) and ΔS (113.67 J mol^{-1} K^{-1}) indicated that SXM adsorption on CBM-A was endothermic and that the degree of freedom at the CBM-A liquid interface increased during SMX adsorption (Nguyen et al., 2025).

Table 2 Thermodynamic parameters for SMX adsorption on SBM-A

Temperature (K)	q_{max} (mg g^{-1})	ΔG (kJ mol^{-1})	ΔH (kJ mol^{-1})	ΔS (J mol^{-1} K^{-1})
288	58.824	-1.52		
298	63.694	-2.58	31.24	113.67
308	65.359	-3.80		

Among the three investigated temperatures, 298 K was selected for the next experiments. This is because 298 K ensures both a relatively high adsorption capacity and economic practical application of CBM-A. Since 298 K is the typical room temperature in summer in Vietnam, it avoids the need to consume energy to increase the temperature to 308 K, thus saving energy.

This justification is supported by other studies, where room temperature (298 K) was also utilized (Ahsan et al., 2018; Sun et al., 2016; Zheng et al., 2013).

3) Adsorption behaviors and mechanisms

3.1) Adsorption kinetics

The experimental data of SMX adsorption on CBM-A were fitted with PFO and PSO kinetic models. The results are presented in Figure 4 and Table 3. On the basis of the qe (mg g-1) and correlation coefficient (R^2) values, the kinetic data for SMX were more satisfactorily described by the PSO kinetic model than by the PFO kinetic model. These findings suggest that SMX adsorption on CBM-A occurred via chemisorption (Ahmed et al., 2017). The PSO kinetic rate constant, k^2, of CBM-A (0.0001) was slightly lower than those of other modified biochars, such as SCA (0.0003) and RCA (0.0005) (Chen et al., 2018).

Table 3 Kinetic parameters for SMX adsorption on CBM-A

Parameters	PFO	PSO
q_e (mg g^{-1})	5.309	1,250.000
k_1 (1 h^{-1}), k_2 (g mg^{-1} h^{-1})	0.0054	0.0001
R^2	0.9024	0.9928

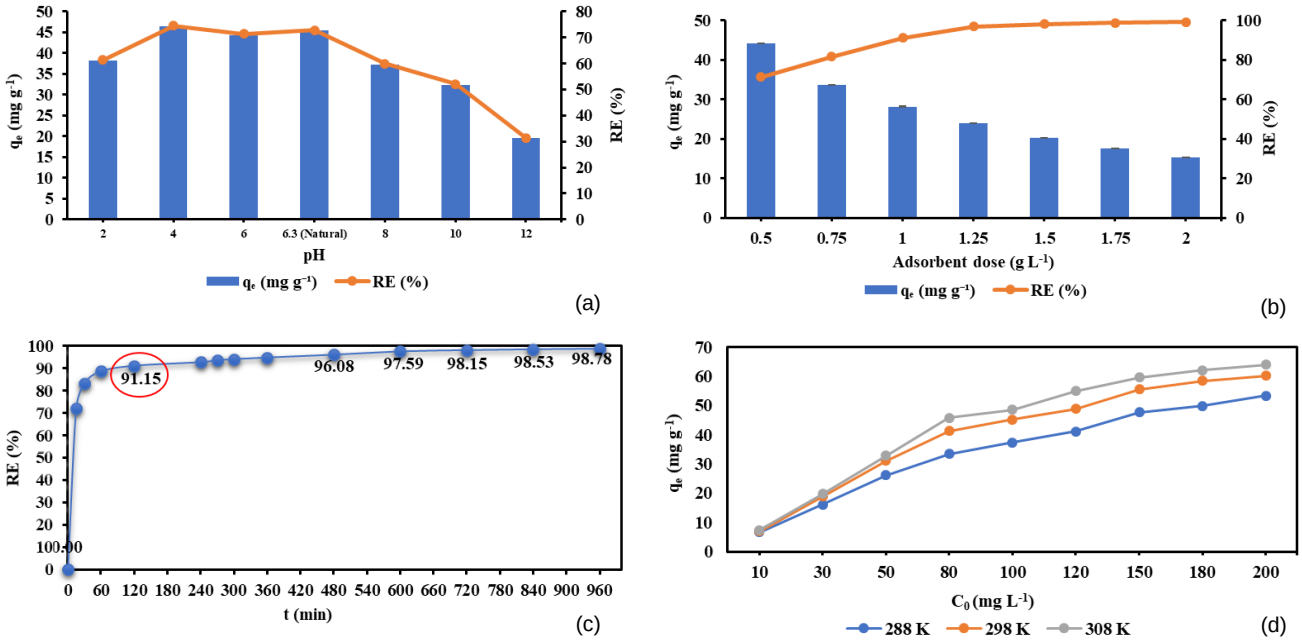

Figure 3 Factors influencing SMX adsorption on CBM-A: a) initial solution pH (2–12), b) CBM-A dose (0.5–2 g L^{-1}), c) contact time (0–960 min), and d) temperature (288, 298, and 308 K).

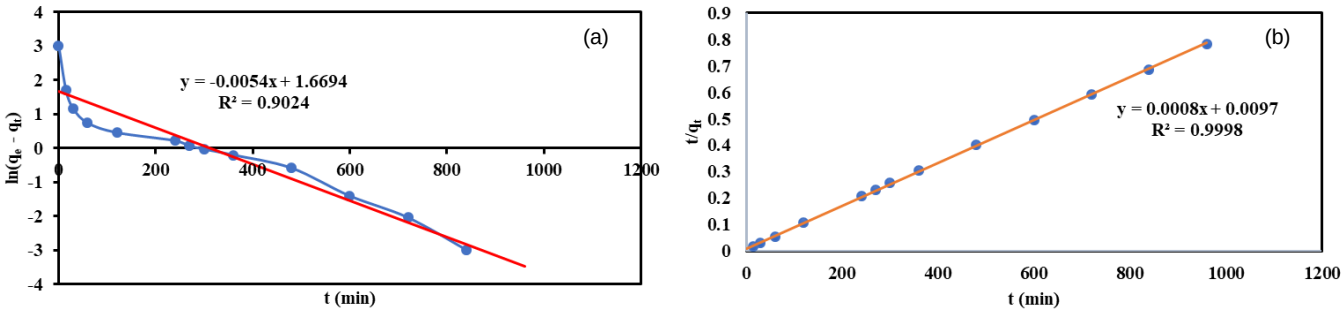

Figure 4 Fitting experimental data for SMX adsorption onto CBM-A with kinetic models: a) Pseudo-first-order (PFO) model and b) Pseudo-second-order (PSO) model.

3.2) Adsorption isotherms

The experimental data for SMX adsorption onto CBM-A were fitted with the Langmuir and Freundlich models, and the results are presented in Figure 5 and Table 4. The Langmuir model (R^2 = 0.9945) was more suitable than the Freundlich model (R^2 = 0.9078) for describing SMX adsorption onto CBM-A because of its higher correlation coefficient. This implies that the adsorption of SMX on CBM-A was characterized by monolayer chemisorption. The SMX q_{max} value of CBM-A (63.29 mg g^{-1}) was more than 5.5-fold greater than that of CB (10.93 mg g^{-1}), indicating that 14% H_3PO_4 acid modification effectively enhanced the SMX adsorption capacity of CB. As shown in Table 5, CBM-A exhibited a superior q_{max} value (63.29 mg g^{-1}) to many pristine biochars (0.16–7.24 mg g^{-1}). Although the q_{max} value of CBM-A for SMX was higher than that of many other biochars (4.91–14.73 mg g^{-1}), it was still lower than that

of SCA (160.3 mg g^{-1}) and RCA (167.5 mg g^{-1}), which were fabricated via the same modification method [1]. This can be attributed to the difference in the substrate categories that were used for the production of the biochars. Moreover, the inferior q_{max} value of CBM-A for SMX compared with that of other biochars modified with other methods (Heo et al., 2019; Zhang et al., 2022) suggests that there is still space for further improvements in the q_{max} value of CBM-A for SMX.

The KF value at 288 K of CBM-A (9.85) was greater than that of the chitosan biochar composites, namely, CTC-OB (2.57) and CTS-SCB (5.57) (Tran et al., 2023). The n value of CBM-A (2.39), which represents the adsorption intensity of CBM-A for SMX, was greater than that of the other modified biochars, namely, SCA (0.15) and RCA (0.13). The n value of CBM-A was greater than 1, indicating that the surface of CBM-A was not uniform, therefore favoring SMX adsorption on CBM-A (Pandiarajan et al., 2018).

Table 4 Isotherm parameters for SMX adsorption on CBM-A

Langmuir model			Freundlich model		
q_{max} (mg g^{-1})	K_L (L mg^{-1})	R^2	K_F ((mg g^{-1})(L mg^{-1})$^{n-1}$)	n	R^2
63.29	0.1042	0.9945	9.85	2.39	0.9078

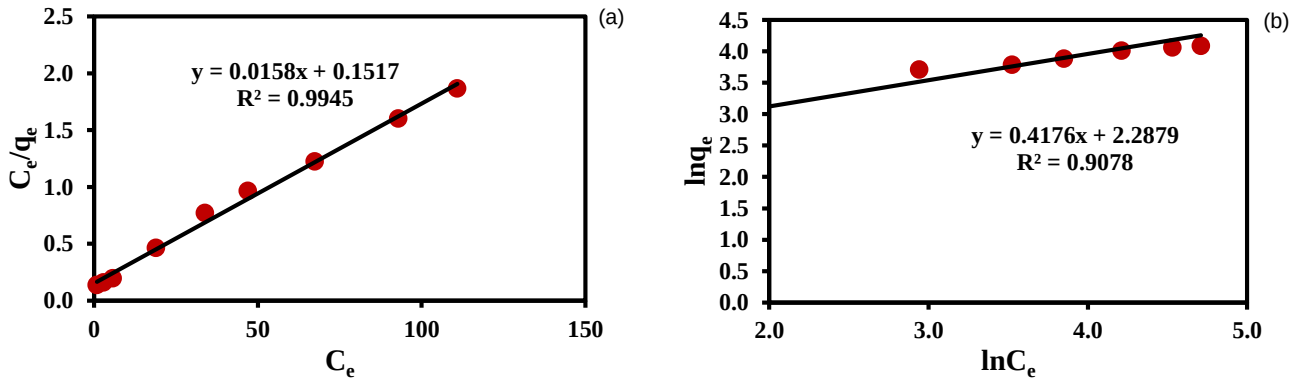

Figure 5 Fitting experimental data for SMX adsorption onto CBM-A with isotherm models: a) Langmuir and b) Freundlich.

4) Regeneration, potential practical application of CBM-A and disposal strategies for CBM-A-SMX

To make CBM-A a viable adsorbent for the treatment of SMX-contaminated wastewater, investigating the desorption, regeneration, and reuse of the spent adsorbent is essential. Although the desorption and regeneration of CBM-A-SMX are outside the scope of this study, a brief literature review of methods lays the foundation for doing so in our future work.

For the desorption of the SMX-spent adsorbent, 0.1 N NaOH was utilized for the desorption of SMX from the spent adsorbent (alfalfa-derived biochar calcined at 650°C for 2 h after saturated adsorption of SMX, namely, AF-650-SMX), with a mass to volume ratio of 0.1 g spent adsorbent to 1 L desorbent. A desorption efficiency of 60–70% was attained in the first 2 h and then reached 75–85% after 24 h (Choi et al., 2019). However, this study did not examine the regeneration and reuse of the SMX desorbed adsorbent. In a more recent study, SMX desorption from spent biochar (produced via the pyrolysis of forest residues via the industrial-scale Terra Fertilis® process) was conducted via a mixture of ethanol and 1 M NaOH (methanol/NaOH = 9:1, v/v) under ultrasonication for 30 min. After that, the SMX removal efficiency of the pristine adsorbent was 99%, whereas that of the regenerated adsorbent remained at 89% after 5 cycles. This method results in not only the effective desorption of SMX and regeneration of the spent adsorbent but also the successful degradation of SMX owing to $SO_4^{\bullet-}$/•OH (Baaloudj et al., 2025). However, the wide application of this method may be restricted by energy consumption and the strong oxidant requirements. Additionally, in both aforementioned studies, SMX-containing NaOH solutions were regenerated, requiring further treatment to avoid secondary pollution. Since CBM-A is similar to both of the above biochars in terms of its lignocellulosic nature, the applicability of these desorption and regeneration methods to CBM-A-SMX should be explored in the future.

Given the limitations of the above desorption and regeneration methods, the development of appropriate disposal strategies is of great interest. Incineration enables the conversion of spent adsorbents as solid waste to energy and mitigates greenhouse gas emissions more than does coal. Additionally, landfilling is another method for disposing of spent adsorbents, provided that the content of antibiotics in the spent adsorbents needs to be determined in advance to evaluate the suitability of the method (Alsawy et al., 2022).

Table 5 Comparison of the q_{max} values for SMX between CBM-A and other biochars

Adsorbent	Modification method	The max adsorption capacity, q_{max} (mg g^{-1})	Reference
Pristine biochars			
Wheat straw biomass BC	-	0.16	Hou et al. (2022)
Orange peel BC	-	3.49	Tran et al. (2023)
Rice straw BC (300 °C)	-	4.21	Sun et al. (2016)
Giant reed BC (300 °C)	-	4.99	Zheng et al. (2013)
Spent coffee ground biochar	-	7.65	Tran et al. (2023)
Corn plant byproducts-derived BC	-	10.93	This study
Modified biochars			
The oxidation-modified BC (O-BC)	Co^{2+}/peroxymonosulfate chemical oxidation	4.91	Hou et al. (2022)
Chitosan orange peel composite (CTS-OB)	Composite	7.24	Tran et al. (2023)
Pine sawdust BC	Oxidative hydrolysis of $FeCl_2$	13.80	Reguyal et al. (2017)
The high-temperature reduction BC (R-BC700)	Reduction at 700 °C	14.66	Hou et al. (2022)
Chitosan spent coffee ground biochar composite (CTS-SCB)	Composite	14.73	Tran et al. (2023)
Functionalized *Eucalyptus* wood-based biochar (fBC)	50% H_3PO_4	28.29	Ahmed et al. (2017)
Acid-modified corn plant byproduct-derived BC	14% H_3PO_4	63.29	This study
Acid-modified swine manure BC (SCA)	14% H_3PO_4	160.3	Chen et al. (2018)
Acid-modified rice straw BC (RCA)	14% H_3PO_4	167.5	Chen et al. (2018)
Wood-derived BC	Boric acid activation	212.87	Zhang et al. (2022)
Bamboo BC composite	Magnetic $CuZnFe_2O_4$	212.87	Heo et al. (2019)

Conclusions

CBM-A was successfully fabricated from corn byproducts by pyrolysis followed by 14% H_3PO_4 acid modification. Acid activation improved the BET surface area and functional groups of CBM-A compared with those of CB. The best SMX abatement from aqueous solutions by CBM-A was achieved at a natural pH of 6.3, a CBM-A dose of 1.5 g L^{-1}, a time of 120 min, and a temperature of 298 K. The maximum adsorption capacity of CBM-A for SMX was 63.29 mg g^{-1}, which was greater than that of many raw and modified biochars from agrowastes. The Langmuir isotherm model (R^2 = 0.9945) and the pseudo-second-order kinetic model (R^2 = 0.9928) satisfactorily described the experimental data for SMX adsorption on CBM-A, suggesting monolayer chemisorption. The thermodynamic results confirmed that SMX adsorption on CBM-A was endothermic and spontaneous. The results show that CBM-A has high potential for application in SMX decontamination in wastewater treatment plants. However, future work should focus on methods for regenerating or treating the spent adsorbent, exploring the potential for adsorbent reuse, and identifying key aspects for the actual application of the adsorbent in wastewater treatment plants.

Acknowledgements

This research has been sponsored by the research project VJU.JICA.RSG.25.04 of VNU Vietnam Japan University.

Data availability statement

Information and data used in the study will be disclosed upon request.

Author ORCID

Nguyen Thi An Hang: 0000-0002-6397-0827

Author contributions

Nguyen Thi An Hang: Conceptualization, Validation, Cata curation, Writing – Review & editing, Supervision, Project administration, Funding acquisition

Le Thi Duyen: Conceptualization, Methodology, Fomal analysis, Investigation, Resources, Writing – Original draft

Bui Thi Hang: Software, Data curation, Writing – Original draft, Visualization

Conflicts of interest

The authors declare that there are no conflicts of interest in competing financial or personal relationships that could have appeared to influence the work reported in this work.

References

Ahmed, M. B., Zhou, J. L., Ngo, H. H., Guo, W., Johir, M. A. H., & Belhaj, D. (2017). Competitive sorption affinity of sulfonamides and chloramphenicol antibiotics toward functionalized biochar for water and wastewater treatment. *Bioresource Technology*, *238*, 306–312.

Ahsan, M. A., Islam, M. T., Imam, M. A., Hyder, A. G., Jabbari, V., Dominguez, N., & Noveron, J. C. (2018). Biosorption of bisphenol A and sulfamethoxazole from water using sulfonated coffee waste: Isotherm, kinetic and thermodynamic studies. *Journal of Environmental Chemical Engineering*, *6*(5), 6602–6611.

Alsawy, T., Rashad, E., El-Qelish, M., & Mohammed, R. H. (2022). A comprehensive review on the chemical regeneration of biochar adsorbent for sustainable wastewater treatment. *NPJ Clean Water*, *5*(1), 29.

Baaloudj, O., Chiron, S., Zizzamia, A. R., Trotta, V., Del Buono, D., Puglia, D., Rallini, M., & Brienza, M. (2025). Efficient biochar regeneration for a circular economy: Removing emerging contaminants for sustainable water treatment. *Colloids and Surfaces A: Physicochemical and Engineering Aspects*, *705*, 135730.

Borowska, E., Felis, E., & Miksch, K. (2015). Degradation of sulfamethoxazole using UV and UV/H_2O_2 processes. *Journal of Advanced Oxidation Technologies*, *18*(1), 69–77.

Chen, T., Luo, L., Deng, S., Shi, G., Zhang, S., Zhang, Y., Deng, O., Wang, L., Zhang, J. & Wei, L. (2018). Sorption of tetracycline on H_3PO_4-modified biochar derived from rice straw and swine manure. *Bioresource Technology*, *267*, 431–437.

Choi, Y. J., Kim, L. H., & Zoh, K. D. (2016). Removal characteristics and mechanism of antibiotics using constructed wetlands. *Ecological Engineering*, *91*, 85–92.

Choi, Y.K., & Kan, E. (2019). Effects of pyrolysis temperature on the physicochemical properties of alfalfa-derived biochar for the adsorption of bisphenol A and sulfamethoxazole in water. *Chemosphere*, *218*, 741–748.

EMA (European Medicines Agency). (2018). *Draft guideline on the environmental risk assessment of medicinal products for human use – revision 1*. EMEA/CHMP/SWP/4447/00 Rev. 1. 2018

Heo, J., Yoon, Y., Lee, G., Kim, Y., Han, J., & Park, C. M. (2019). Enhanced adsorption of bisphenol A and sulfamethoxazole by a novel magnetic $CuZnFe_2O_4$–biochar composite. *Bioresource Technology*, *281*, 179–187.

Hou, J., Yu, J., Li, W., He, X., & Li, X. (2022). The effects of chemical oxidation and high-temperature reduction on surface functional groups and the adsorption performance of biochar for sulfamethoxazole adsorption. *Agronomy*, *12*(2), 510.

Jang, H. M., Yoo, S., Choi, Y. K., Park, S., & Kan, E. (2018). Adsorption isotherm, kinetic modeling and mechanism of tetracycline on Pinus taeda-derived activated biochar. *Bioresource Technology*, *259*, 24–31.

Jia, Z., Zeng, W., Xu, H., Li, S., & Peng, Y. (2020). Adsorption removal and reuse of phosphate from wastewater using a novel adsorbent of lanthanum-modified platanus biochar. *Process Safety and Environmental Protection*, *140*, 221–232.

Liu, S., Wang, N., Li, Y., Liang, D., He, W., Lin, N., Li, J., & Feng, Y. (2025). Magnetic biochar-mediated iron reduction synergizes with microbial co-metabolism for enhanced adsorption and in-situ degradation of sulfamethoxazole. *Chemical Engineering Journal*, *523*, 168620.

Nguyen, T. A. H., Nguyen, Q. H., Bui, T. H., & Do, D. Q. (2025). Acid-activated shrimp shell-derived hydrochar for adsorptive removal of anionic direct blue 71 dye from aqueous solutions. *Journal of Water and Environment Technology*, *23*(1), 1–15.

Niegowska, M., Sanseverino, I., Navarro, A., & Lettieri, T. (2021). Knowledge gaps in the assessment of antimicrobial resistance in surface waters. *FEMS Microbiology Ecology*, *97*(11), fiab140.

Pandiarajan, A., Kamaraj, R., Vasudevan, S., & Vasudevan, S. (2018). OPAC (orange peel activated carbon) derived from waste orange peel for the adsorption of chlorophenoxyacetic acid herbicides from water: adsorption isotherm, kinetic modelling and thermodynamic studies. *Bioresource Technology*, *261*, 329–341.

Peng, H., Gao, P., Chu, G., Pan, B., Peng, J., & Xing, B. (2017). Enhanced adsorption of Cu (II) and Cd (II) by phosphoric acid-modified biochars. *Environmental Pollution*, *229*, 846–853.

Reguyal, F., Sarmah, A. K., & Gao, W. (2017). Synthesis of magnetic biochar from pine sawdust via oxidative hydrolysis of $FeCl_2$ for the removal of sulfamethoxazole from aqueous solution. *Journal of Hazardous Materials*, *321*, 868–878.

Sun, B., Lian, F., Bao, Q., Liu, Z., Song, Z., & Zhu, L. (2016). Impact of low molecular weight organic acids (LMWOAs) on biochar micropores and sorption properties for sulfamethoxazole. *Environmental Pollution*, *214*, 142–148.

Taheri, M. A. R., Astaraei, A. R., Lakzian, A., & Emami, H. (2024). The role of biochar and sulfur-modified

biochar on soil water content, biochemical properties and millet crop under saline-sodic and calcareous soil. *Plant and Soil*, *499*(1), 221–236.

Tran, V. S., Ngo, H. H., Guo, W., Nguyen, T. H., Luong, T. M. L., Nguyen, X. H., Phan, T. L. A., Le, V. T., Nguyen, M. P. & Nguyen, M.K. (2023). New chitosan-biochar composite derived from agricultural waste for removing sulfamethoxazole antibiotics in water. *Bioresource Technology*, *385*, 129384.

Zhang, X., Gang, D.D., Zhang, J., Lei, X., Lian, Q., Holmes, W.E., Zappi, M. E., & Yao, H. (2022). Insight into the activation mechanisms of biochar by boric acid and its application for the removal of sulfamethoxazole. *Journal of Hazardous Materials*, *424*, 127333.

Zhang, Y., Liu, Y., Li, Y., Cheng, H., Zhu, C., Shen, Y., Shao, S., Xue, J., Zhou, D., & Cao, F. (2025). Cost-effective micro/mesoporous biochar derived from soda residue-assisted hydrocarbonization and activation of crop waste for sulfamethoxazole removal from water environments. *Bioresource Technology*, *437*, 133166.

Zheng, H., Wang, Z., Zhao, J., Herbert, S., & Xing, B. (2013). Sorption of antibiotic sulfamethoxazole varies with biochars produced at different temperatures. *Environmental Pollution*, *181*, 60–67.

Zhou, L., Deng, H., Zhang, W., & Gao, Y. (2015). Photodegradation of sulfamethoxazole and photolysis active species in water under Uv-Vis light irradiation. *Fresenius Environmental Bulletin*, *24*(5), 1685–1691.

Zhou, Y., Liu, X., Xiang, Y., Wang, P., Zhang, J., Zhang, F., Wei, J., Luo, L., Lei, M., & Tang, L. (2017). Modification of biochar derived from sawdust and its application in removal of tetracycline and copper from aqueous solution: Adsorption mechanism and modelling. *Bioresource Technology*, *245*, 266–273.